Scientia Iranica A (2014) 21(5), 1549–1565

SCIENTIA IRANICA

Sharif University of Technology
Scientia Iranica
Transactions A: Civil Engineering
www.scientiairanica.com

Analytical reliability assessment of liquefaction potential based on cone penetration test results

A. Johari* **and A.R. Khodaparast**

Department of Civil and Environmental Engineering, Shiraz University of Technology, Shiraz, Iran.

Received 29 May 2013; received in revised form 7 December 2013; accepted 3 February 2014

KEYWORDS
Reliability;
Jointly distributed random variables method;
Monte Carlo simulation;
Liquefaction;
Standard penetration test.

Abstract. Determination of site liquefaction potential and subsequent deterrent action can prevent significant damage to structures. In this way, a probabilistic liquefaction assessment can develop potential flexibility and risk management decisions. Based on the advantage of probabilistic assessment, considerable research has been carried out in the past few years on liquefaction potential. In this research, the jointly distributed random variables method is used as an analytical method for probabilistic analysis and reliability assessment of liquefaction potential based on cone penetration test results. The selected stochastic parameters are corrected CPT tip resistance and the stress reduction factor, which are modeled using a truncated normal probability density function and peak horizontal earthquake acceleration ratio and magnitude, which are considered to have a truncated exponential probability density function. The depth of the water table and fines content are regarded as constant parameters. The results are compared with those of the Monte Carlo simulation. Comparison of the results and parametric analysis indicates the very good performance of the proposed approach in the assessment of reliability. A sensitivity analysis shows that the moment magnitude is the most effective parameter in soil liquefaction potential.

1. Introduction

Predicting the liquefaction resistance of soils is an important aspect of geotechnical earthquake engineering practice. During an earthquake, significant damage can result due to the instability of the soil in the area affected by internal seismic waves. Liquefaction is known as one of the major causes of ground failure related to earthquakes. It is believed to occur when the pore pressure approaches the confining pressure in loose, saturated sands under earthquake loading where, as a result of a rapid and dramatic loss of soil strength, it can initiate the movement of large blocks of soil causing extensive damage to civil engineering structures.

The stress-based simplified procedure, originated by Seed and Idriss [1], is widely used by geotechnical engineers for assessing the liquefaction potential of soils in an earthquake. This simplified procedure requires evaluation of the seismic loading in terms of Cyclic Stress Ratio (CSR), as defined by the pioneering work of Seed and Idriss [1], and liquefaction resistance in terms of the Cyclic Resistance Ratio (CRR) [2]. Because of the difficulty of sampling, CRR is generally determined with simplified methods, such as Standard Penetration Test (SPT)-based methods [3-8], Cone Penetration Test (CPT)-based methods [3,6,8-15], and shear wave velocity (Vs)-based methods [3,16,17].

The Cone Penetration Test (CPT) has been

*. *Corresponding author.*
E-mail addresses: johari@sutech.ac.ir (A. Johari); a.khodaparast@sutech.ac.ir (A.R. Khodaparast)

widely used for the last twenty years as a site investigation tool. The CPT has major advantages over traditional methods of field site investigation, such as drilling and sampling, since it is fast, repeatable and economical. In addition, it provides near continuous data and has a strong theoretical background. These advantages have led to a steady increase in the use and application of the CPT all around the world. Because of the inherent variability of most soil deposits, the continuous nature of CPT data is extremely valuable.

The inherent uncertainties of characteristics which affect liquefaction dictate that this problem is of a probabilistic nature rather than being deterministic. Uncertainty in liquefaction can be divided into two distinctive categories: uncertainty in the cyclic stress ratio due to earthquake characteristics, and uncertainty in the cyclic resistance ratio due to soil properties. In the first category, the selection of appropriate earthquake parameters, such as magnitude, location and recurrence, to assess the liquefaction potential of the site is important, and in the second category, parameter uncertainty, model uncertainty and human uncertainty are important [18]. Parameter uncertainty is the uncertainty in the input parameters for analysis [19], model uncertainty is due to the limitation of the theories and models used in performance prediction [20], while human uncertainty is due to human error [21]. In this research, only parameter uncertainty is assessed.

Reliability analysis provides a means of evaluating the combined effects of uncertainties and offers a logical framework for choosing factors of safety that are appropriate for the degree of uncertainty and the consequences of failure. Thus, as an alternative or as a supplement to deterministic assessment, a reliability assessment of liquefaction potential would be useful in providing better engineering decisions.

There are many reliability approaches that have been developed to deal with uncertainties in liquefaction potential. These approaches can be grouped into five categories: analytical methods, approximate methods, Monte Carlo simulation, logistic regression methods and artificial intelligence methods.

1. In analytical methods, the probability density functions of input variables are expressed mathematically. They are then integrated analytically into the safety factor relationship for liquefaction to derive a mathematical expression for the density function of the factor of safety. Limited attempts have been made to apply analytical methods. The jointly distributed random variables method lies in this category. Recent research has been undertaken to apply this method to the reliability assessment of liquefaction potential based on triaxial test results [22] and standard penetration tests [23].
2. Most approximate methods are modified versions of three methods, namely, First Order Second Moment (FOSM) method [24], Point Estimate Method (PEM) [25], and First Order Reliability Method (FORM) [26]. These approaches require the mean and variance of stochastic input variables, as well as the performance function that defines the liquefaction safety factor [27-37].
3. Monte Carlo simulation uses randomly generated points to cover the range of values that enter into a calculation [38]. As many as 100,000 to 1,000,000 generation points may be required to adequately represent a deterministic solution. The computation of probabilities by Monte Carlo simulation is a procedure commonly adopted to solve problems that are not readily solved by analytical methods [39-41].
4. The rationality of the reliability analysis results largely depends on the amount and quality of the collected data used to deduce the statistics of the cyclic soil strength. Several researchers have established probabilistic cyclic strength curves by the logistic regression method. This method requires collecting data for liquefaction and non-liquefaction cases [42-46].
5. Artificial intelligence method: In recent years, by pervasive developments in computational software and hardware, several alternative computer-aided pattern recognition approaches have emerged. The main idea behind pattern recognition systems, such as neural network, fuzzy logic or genetic programming, is that they learn adaptively from experience and extract various discriminates, each appropriate for its purpose. Artificial Neural Networks (ANNs) and Multi-Layer Regression (MLR) are the most widely used pattern recognition procedures that have been introduced for determination of liquefaction potential. In this approach, the reliability analysis is done based on a function that is developed by an appropriate artificial intelligence method [13,47-52].

In analytical methods, the derivation is done only once and, after that, it can be used in many applications. It is also worth noting that, in some problems such as liquefaction potential assessment, when a relatively large number of variables are involved, the Monte Carlo method may require hundreds of thousands of simulation runs that make the method excessively demanding in computational time and resources. Moreover, the jointly distributed random variables method, which is employed as an analytical method in this research, can be used for stochastic parameters with any distribution curve (such as normal, exponential, gamma, uniform,...), whereas some methods like PEM, and FOSM, require specific (e.g., normal) distribution functions. This ability is very important because the peak horizontal earthquake acceleration ratio (α) and earthquake magnitude (M_w), which are presented in the liquefaction potential relationship, are considered to have truncated exponential probability density functions. Based on these advantages, in this research, the jointly distributed random variables method is used to assess the reliability of the safety factor in the prediction of liquefaction potential considering the uncertainties in parameters.

2. Assessment of liquefaction potential using CPT results

The Factor of Safety (FS) against liquefaction in terms of Cyclic Resistance Ratio for earthquakes with magnitude of 7.5 (CRR7.5), Cyclic Stress Ratio (CSR), earthquake Magnitude Scaling Factor (MSF), and overburden stress correction factor (K_σ) is defined by:

$$\mathrm{FS}=\frac{\mathrm{CRR}_{7.5}}{\mathrm{CSR}}.\mathrm{MSF}.\mathrm{K}_\sigma. \tag{1}$$

No liquefaction is predicted if FS $>$ 1. On the other hand, if FS $\leq$ 1, liquefaction is predicted.

Idriss and Boulanger [15] proposed the following relation for calculating CRR7.5 from CPT results:

$$\mathrm{CRR}_{7.5}=\exp\left\{\frac{(q_{c1N})_{\mathrm{cs}}}{540}+\left(\frac{(q_{c1N})_{\mathrm{cs}}}{67}\right)^2-\left(\frac{(q_{c1N})_{\mathrm{cs}}}{80}\right)^3+\left(\frac{(q_{c1N})_{\mathrm{cs}}}{114}\right)^4-3\right\}, \tag{2}$$

where $(q_{c1N})_{\mathrm{cs}}$ is the clean-sand equivalent of the corrected CPT tip aresistance, q_{c1N}, defined as [53]:

$$(q_{c1N})_{\mathrm{cs}}=q_{c1N}+\Delta q_{c1N}, \tag{3}$$

$$\Delta q_{c1N}=\left(5.4+\frac{q_{c1N}}{16}\right).\exp\left(1.63+\frac{9.7}{\mathrm{FC}+0.01}-\left(\frac{15.7}{\mathrm{FC}+0.01}\right)^2\right), \tag{4}$$

where q_{c1N} is the corrected CPT tip resistance normalized to the effective overburden stress of 100 kPa, and FC is fine content (%).

The Cyclic Stress Ratio (CSR) is generally obtained from the simplified procedure originally proposed by Seed and Idriss [1] as:

$$\mathrm{CSR}=(\frac{\tau_{\mathrm{av}}}{\sigma_v'})=0.65(\frac{\sigma_v}{\sigma_v'})(\frac{a_{\max}}{g})(r_d), \tag{5}$$

where:

σ_v'	Effective vertical stress;
σ_v	Total vertical stress;
τ_{av}	Average shear stress causing liquefaction;
$(a_{\max}/g)=\alpha$	Peak horizontal ground surface acceleration normalized with respect to acceleration of gravity;
r_d	Stress reduction factor.

The stress reduction factor, r_d, provides an approximate correction for flexibility in the soil profile. There are several empirical relations for determination of r_d. The earliest and most widely used recommendation for assessment of r_d was proposed by Seed and Idriss [1], approximated by Liao and Whitman [54], and expressed by Youd and Idriss [3] as:

$$r_d=\frac{1.0-0.4113\mathrm{h}^{0.5}+0.04052\mathrm{h}+0.001753\mathrm{h}^{1.5}}{1.0-0.4177\mathrm{h}^{0.5}+0.05729\,\mathrm{h}-0.006205\,\mathrm{h}^{1.5}+0.00121\mathrm{h}^2}, \tag{6}$$

where h is the depth below ground surface (m). The magnitude scaling factor, MSF, has been used to adjust the induced CSR during earthquake magnitude, M_w, to an equivalent CSR for an earthquake magnitude, $M_w=7.5$. The MSF is, thus, expressed as [3]:

$$\mathrm{MSF}=\left(\frac{M_w}{7.5}\right)^{-2.56}, \tag{7}$$

where M_w is the moment magnitude. Overburden pressure correction factor, K_σ, is used to adjust the cyclic resistance ratio, where the overburden stresses are much greater than 100 kPa. This factor is defined by Idriss and Boulanger [15] as below:

$$K_\sigma=1-C_\sigma\ln(\sigma_v'/P_a)\leq 1.0, \tag{8}$$

where:

$$C_\sigma=\frac{1}{18.9-17.2D_R}\leq 0.3. \tag{9}$$

P_a is the atmospheric air pressure; and D_R is the field relative density.

Eq. (1) can be rewritten based on Eqs. (2) to (9) as in Eq. (10) shown in Box I. Eq. (10) can be simplified as follows:

$$\mathrm{FS}(q_{c1N},r_d,\alpha,M_w)=\frac{L(q_{c1N}).M_w^{-2.56}}{r_d.\alpha}. \tag{11}$$

$L(q_{c1N})$ is obtained by Eq. (12) as shown in Box II. It is noted that if $\sigma_v'\leq 100$ kPa, then $K_\sigma=1.0$ and the term of $\left(1-\frac{1}{(18.9-17.3D_R)}\ln\left(\frac{(\gamma_{\mathrm{sat}}-\gamma_w)h}{P_a}\right)\right)$ is removed from Eq. (12).

$$\mathrm{FS}=\frac{\exp\left\{\frac{(q_{c1N})_{\mathrm{cs}}}{540}+\left(\frac{(q_{c1N})_{\mathrm{cs}}}{67}\right)^2-\left(\frac{(q_{c1N})_{\mathrm{cs}}}{80}\right)^3+\left(\frac{(q_{c1N})_{\mathrm{cs}}}{114}\right)^4-3\right\}\left(1-\frac{1}{18.9-17.3D_R}\ln(\frac{\sigma'_v}{P_a})\right)}{0.65\frac{\sigma_v}{\sigma'_v}\times\frac{a_{\max}}{g}\times r_d\times(M_w/7.5)^{2.56}}$$

$$=\frac{\exp\left\{\frac{q_{c1N}+\Delta q_{c1N}}{540}+\left(\frac{q_{c1N}+\Delta q_{c1N}}{67}\right)^2-\left(\frac{q_{c1N}+\Delta q_{c1N}}{80}\right)^3+\left(\frac{q_{c1N}+\Delta q_{c1N}}{114}\right)^4-3\right\}}{\frac{0.65\times\gamma_{\mathrm{sat}}\times\alpha\times r_d\times(M_w/7.5)^{2.56}}{(\gamma_{\mathrm{sat}}-\gamma_w)\left(1-\frac{1}{18.9-17.3D_R}\ln\left(\frac{(\gamma_{\mathrm{sat}}-\gamma_w)h}{P_a}\right)\right)}} \quad (10)$$

Box I

$$L(q_{c1N})=\frac{\exp\left\{\frac{q_{c1N}+\Delta q_{c1N}}{540}+\left(\frac{q_{c1N}+\Delta q_{c1N}}{67}\right)^2-\left(\frac{q_{c1N}+\Delta q_{c1N}}{80}\right)^3+\left(\frac{q_{c1N}+\Delta q_{c1N}}{114}\right)^4-3\right\}}{\frac{0.65\times\gamma_{\mathrm{sat}}}{7.5^{2.56}(\gamma_{\mathrm{sat}}-\gamma_w)\left(1-\frac{1}{(18.9-17.3D_R)}\ln\left(\frac{(\gamma_{\mathrm{sat}}-\gamma_w)h}{P_a}\right)\right)}} \quad (12)$$

Box II

3. Developing relations between dependent variables

The jointly distributed random variables method that is used for reliability assessment in this research assumes that the variables are independent. There are several stochastic parameters in Eqs. (11) and (12). As the liquefaction classification problem is highly nonlinear in nature, it is difficult to develop a comprehensive model taking into account all the independent variables, such as the seismic and soil properties, using conventional modeling techniques. Hence, in many of the conventional methods that have been proposed, simplified assumptions have been made.

No direct correlation exists between α and earthquake magnitude. Several empirical relationships have been developed for estimating α as a function of earthquake magnitude, distance from the seismic energy source, and local site conditions. Preliminary attenuation relationships have also been developed for a limited range of soft soil sites by Idriss [55]. Selection of an attenuation relationship should be based on such factors as the region of the country, type of faulting, and site condition [3].

On the other hand, in Eq. (12), parameters D_R and γ_{sat} are related to q_{c1N}. In this section, the relationship between D_R and q_{c1N}, as well as γ_{sat} and q_{c1N}, is developed to resolve the dependency problem of variables in this equation. As a result of this derivation, Eq. (11) has four independent stochastic parameters: peak ground acceleration (α), Moment magnitude (M_w), corrected CPT tip resistance (q_{c1N}), and stress reduction factor (r_d), as well as assumed deterministic parameters average Fines Content (FC), maximum possible dry unit weight ($\gamma_{d_{\max}}$), minimum possible dry unit weight ($\gamma_{d_{\min}}$), water unit weight (γ_w), and specific gravity (G_s).

3.1. Relation between D_R and q_{c1N}

Andrus et al. [56] proposed the following relation between $N_{1,60\mathrm{cs}}$ and q_{c1Ncs}:

$$N_{1,60\mathrm{cs}}=0.356(q_{(c1N)_{\mathrm{cs}}})^{0.851}, \quad (13)$$

where $N_{1,60\mathrm{cs}}$ is the clean-sand equivalent of the overburden stress-corrected SPT blow count, which can be calculated from Eq. (3); and $q_{c1N\mathrm{cs}}$ is the clean-sand equivalent of the overburden stress-corrected CPT tip resistance [3], defined as:

$$N_{1,60\mathrm{cs}}=a+b.N_{1,60}, \quad (14)$$

where $N_{1,60}$ is the corrected SPT blow count normalized to the effective overburden stress of 100 kPa; a and b are the coefficients to account for the effect of Fines Content (FC), defined by [3]:

$$\begin{cases} a=0 & \mathrm{FC}\leq 5\% \\ a=\exp[1.76-(190/\mathrm{FC}^2)] & 5\%<\mathrm{FC}<35\% \\ a=5.0 & \mathrm{FC}\geq 35\% \end{cases} \quad (15)$$

$$\begin{cases} b=1 & \mathrm{FC}\leq 5\% \\ b=\exp[0.99+(\mathrm{FC}^{1.5}/1000)] & 5\%<\mathrm{FC}<35\% \\ b=1.2 & \mathrm{FC}\geq 35\% \end{cases} \quad (16)$$

Several relationships between relative density and

SPT blow counts have been proposed in the literature [53,57,58]. Cubrinovski and Ishihara [59] proposed a relationship between DR and corrected SPT blow count as expressed in Eq. (17):

$$D_R = \sqrt{\frac{N_{1,60}}{C_D}}, \tag{17}$$

where:

$$C_D = \frac{9}{(e_{\max} - e_{\min})^{1.7}}, \tag{18}$$

where $e_{\max}$ is the maximum possible void ratio from laboratory experiment; and $e_{\min}$ is the minimum possible void ratio from laboratory experiment.

The void ratio range ($e_{\max} - e_{\min}$) can be calculated as [60]:

$$e = \frac{G_s \gamma_w}{\gamma_d} - 1 \rightarrow \begin{Bmatrix} e_{\max} = \frac{G_s\gamma_w}{\gamma_{d_{\min}}} - 1 \\ e_{\min} = \frac{G_s\gamma_w}{\gamma_{d_{\max}}} - 1 \end{Bmatrix}$$

$$\rightarrow e_{\max} - e_{\min} = \frac{G_s \gamma_w (\gamma_{d_{\max}} - \gamma_{d_{\min}})}{\gamma_{d_{\max}} . \gamma_{d_{\min}}}, \tag{19}$$

where $\gamma_{d_{\max}}$ is the maximum possible dry unit weight from laboratory experiment; and $\gamma_{d_{\min}}$ is the minimum possible dry unit weight from laboratory experiment.

Using Eqs. (13) to (19), Eq. (17) can be rewritten in Eq. (20) as shown in Box III.

3.2. Relation between γ_{sat} and q_{c1N}

The relation between γ_{sat} and γ_d can be derived from their basic definitions as [60]:

$$\begin{cases} \gamma_{\text{sat}} = \frac{(G_s + e)\gamma_w}{1+e} \\ \gamma_d = \frac{G_s \times \gamma_w}{1+e} \quad \rightarrow \quad e = \frac{G_s \times \gamma_w}{\gamma_d} - I \end{cases}$$

$$\rightarrow \quad \gamma_{\text{sat}} = \frac{\left(G_s\left(1 + \frac{\gamma_w}{\gamma_d}\right) - 1\right)\gamma_d}{G_s}, \tag{21}$$

where:

γ_{sat} Saturated unit weight;

γ_d Dry unit weight in natural state of soil;

G_s Specific gravity of soil solids;

γ_w Unit weight of water (9.81 kN/m^3);

e Void ratio in natural state of soil.

The relation between relative density (D_R) and dry unit weight (γ_d) is [60]:

$$D_R = \frac{\gamma_d - \gamma_{d_{\min}}}{\gamma_{d_{\max}} - \gamma_{d_{\min}}} \times \frac{\gamma_{d_{\max}}}{\gamma_d}$$

$$\rightarrow \quad \gamma_d = \frac{\gamma_{d_{\min}} . \gamma_{d_{\max}}}{\gamma_{d_{\max}} - D_R(\gamma_{d_{\max}} - \gamma_{d_{\min}})}. \tag{22}$$

Using Eqs. (21) and (22), the relation between γ_{sat} and D_R can be developed as follows:

$$\gamma_{\text{sat}} = \frac{\gamma_{d_{\max}} . \gamma_{d_{\min}} (G_s - 1)}{G_s\left(\gamma_{d_{\max}} + (\gamma_{d_{\min}} - \gamma_{d_{\max}})D_R\right)}. \tag{23}$$

Substituting Eq. (20) in Eq. (23), the relation between γ_{sat} and q_{c1N} can be developed by Eq. (24) as shown in Box IV.

Substituting Eqs. (20) and (24) into Eqs. (11) and (12), these equations convert to a stochastic independent variable relations.

4. Jointly distributed random variables method

Jointly Distributed Random Variables (JDRV) method is an analytical probabilistic method. In this method, the density function of input variables are expressed mathematically and jointed together by statistical relations. The jointly distributed random variables method has a number of advantages over other methods:

(i) It is an exact method and can be used for stochastic parameters with any distribution curve (such as normal, exponential, gamma and uniform), whereas, some methods, like Point Estimated Method (PEM), and First Order Second Moment (FOSM), require specific (e.g., normal) distribution functions.

(ii) The computational time of this method is significantly less than the Monte Carlo simulation (MCs), which requires a significant number of simulation runs.

The available statistical and probabilistic relations between random variables are given in this section [61-63]. Recent research has been undertaken to apply this method to geotechnical problems [22,23,64-67].

$$D_R = \sqrt{\frac{0.356(q_{c1N} + \Delta q_{c1N})^{0.851} - a}{b.C_D}} = \sqrt{\left(\frac{0.356}{9b}(q_{c1N} + \Delta q_{c1N})^{0.851} - \frac{a}{9b}\right)\left(\frac{G_s\gamma_w(\gamma_{d_{\max}} - \gamma_{d_{\min}})}{\gamma_{d_{\max}} . \gamma_{d_{\min}}}\right)^{1.7}} \tag{20}$$

Box III

$$\gamma_{\text{sat}} = \frac{\gamma_{d_{\max}}.\gamma_{d_{\min}}(G_s-1)}{G_s\left(\gamma_{d_{\max}}+(\gamma_{d_{\min}}-\gamma_{d_{\max}})\sqrt{\frac{0.356(q_{c1N}+\Delta q_{c1N})^{0.851}-a}{b.C_D}}\right)} =$$
$$\frac{\gamma_{d_{\max}}.\gamma_{d_{\min}}(G_s-1)}{G_s\left(\gamma_{d_{\max}}+(\gamma_{d_{\min}}-\gamma_{d_{\max}})\sqrt{\left(\frac{0.356}{9b}(q_{c1N+\Delta q_{c1N}})^{0.851}-\frac{a}{9b}\right)\left(\frac{G_s\gamma_w(\gamma_{d_{\max}}-\gamma_{d_{\min}})}{\gamma_{d_{\max}}.\gamma_{d_{\min}}}\right)^{1.7}}\right)}. \tag{24}$$

Box IV

Theorem 1. If X is a random variable with the probability density of $f_X(x)$, and Y is a function of X in the form $Y = g(x)$, the probability density of Y can be determined as:

$$f_Y(y) = f_X(g^{-1}(y)) \times \left|\frac{dg^{-1}(y)}{dy}\right|$$
$$= f_X(X) \times \left|\frac{1}{\frac{dy}{dx}}\right|. \tag{25}$$

This relation is valid for the monotonically increasing or decreasing function, $g(x)$.

Theorem 2. If X and Y are two independent random variables with the probability densities $f_X(x)$ and $f_Y(y)$, and $Z = X + Y$, the probability density of Z will be:

$$f_{X+Y}(Z) = \int_{-\infty}^{+\infty} f_X(X)f_Y(Z-X)dx,$$
$$-\infty < Z < +\infty. \tag{26}$$

Theorem 3. If X and Y are two independent random variables with the probability densities $f_X(x)$ and $f_Y(y)$, and $Z = X - Y$, the probability density of Z will be:

$$f_{X-Y}(Z) = \int_{-\infty}^{+\infty} f_X(X)f_Y(X-Z)dx,$$
$$-\infty < Z < +\infty. \tag{27}$$

Theorem 4. If X and Y are two independent random variables with the probability densities $f_X(x)$ and $f_Y(y)$, and $Z = Y/X$, the probability density of Z will be calculated as:

$$f_{Y/X}(Z) = \int_{-\infty}^{+\infty} |X| f_X(X)f_Y(X.Z)dx,$$
$$-\infty < Z < +\infty. \tag{28}$$

Theorem 5. If X and Y are two independent random variables with the probability densities $f_X(x)$ and $f_Y(y)$, and $Z = X.Y$, the probability density of Z will be calculated as:

$$f_{X.Y}(Z) = \int_{-\infty}^{+\infty} \left|\frac{1}{X}\right| f_X(X)f_Y\left(\frac{Z}{X}\right)dx,$$
$$-\infty < Z < +\infty. \tag{29}$$

5. Monte Carlo simulation

The simulation by Monte Carlo can solve problems by generating suitable random numbers (or pseudo-random numbers) and assessing the dependent variable for a large number of possibilities. The Monte Carlo simulation (MCs) involves the definition of variables that generate uncertainty and probability density function (pdf), determination of the value of the function using variable values randomly obtained considering the pdf, and repeating this procedure until acquiring a sufficient number of outputs to build the pdf of the function. The minimum number of trials [68] can be estimated from:

$$N = \left(\frac{100d}{E}\right)^2 \frac{1-P_f}{P_f}m, \tag{30}$$

where:

N	Number of Monte Carlo trials;
P_f	Probability of unsatisfactory performance;
E	Relative percent error in estimating P_f;
m	Number of component random variables;
d	Normal standard deviate with confidence levels.

6. Reliability assessment by jointly distributed random variables method

To assess reliability and account for uncertainties in liquefaction potential, four independent input parameters have been defined as stochastic variables. The stochastic parameters are corrected CPT tip resistance (q_{c1N}) and stress reduction factor (r_d), which are modeled using truncated normal probability density functions (pdf), the peak horizontal earthquake acceleration ratio (α) and earthquake magnitude (M_w), which are considered to have truncated exponential probability density functions. The depth is regarded as a constant parameter. The distribution functions for the above mentioned stochastic parameters are as follows:

$$f_{q_{c1N}}(q_{c1N}) = \frac{1}{\sigma_{q_{c1N}}\sqrt{2\pi}} \exp\left(-0.5\left(\frac{q_{c1N} - q_{c1N\text{mean}}}{\sigma_{q_{c1N}}}\right)^2\right),$$

$$q_{c1N\min} \leq q_{c1N} \leq q_{c1N\max}, \tag{31}$$

$$f_{r_d}(r_d) = \frac{1}{\sigma_{r_d}\sqrt{2\pi}} \exp\left(-0.5\left(\frac{r_d - r_{d_{\text{meam}}}}{\sigma_{r_d}}\right)^2\right),$$

$$r_{d_{\min}} \leq r_d \leq r_{d_{\max}}, \tag{32}$$

$$f_\alpha(\alpha) = \frac{\lambda_\alpha.\exp(-\lambda_\alpha.\alpha)}{\exp(-\lambda_\alpha.\alpha_{\min}) - \exp(-\lambda_\alpha.\alpha_{\max})},$$

$$\alpha_{\min} \leq \alpha \leq \alpha_{\max}, \tag{33}$$

$$f_{M_w}(M_w) = \frac{\lambda_{M_w}.\exp(-\lambda_{M_w}.M_w)}{\exp(-\lambda_{M_w}.M_{w_{\min}}) - \exp(-\lambda_{M_w}.M_{w_{\max}})}$$

$$M_{w_{\min}} \leq M_w \leq M_{w_{\max}}, \tag{34}$$

where:

$$\begin{cases} q_{c1N_{\min}} = q_{c1N_{\text{mean}}} - 4\sigma_{q_{c1N}} \\ q_{c1N_{\max}} = q_{c1N_{\text{mean}}} - 4\sigma_{q_{c1N}} \end{cases} \tag{35}$$

$$\begin{cases} r_{d_{\min}} = r_{d_{\text{mean}}} - 4\sigma_{r_d} \\ r_{d_{\max}} = r_{d_{\text{mean}}} - 4\sigma_{r_d} \end{cases} \tag{36}$$

$q_{c1N_{\text{mean}}}$	Average value of corrected CPT tip resistance;
σ_{qc1N}	Standard deviation of corrected SPT blow count;
$q_{c1N_{\min}}$	Minimum value of corrected SPT blow count;
$q_{c1N_{\max}}$	Maximum value of corrected SPT blow count;
$r_{d_{\text{mean}}}$	Average value of stress reduction factor;
σ_{r_d}	Standard deviation of stress reduction factor;
$r_{d_{\min}}$	Minimum value of stress reduction factor;
$r_{d_{\max}}$	Maximum value of stress reduction factor;
$\alpha_{\min}$	Minimum value of earthquake acceleration ratio;
$\alpha_{\max}$	Maximum value of earthquake acceleration ratio;
λ_α	Rate of change in earthquake acceleration ratio (rate parameter) $=1/\beta_\alpha$;
β_α	Scale parameter of earthquake acceleration ratio;
$M_{W_{\min}}$	Minimum value of moment magnitude;
$M_{W_{\max}}$	Maximum value of moment magnitude;
λ_{M_w}	Rate of change in moment magnitude (rate parameter) $=1/\beta_{M_w}$;
β_{M_w}	Scale parameter of moment magnitude.

By considering the stochastic variables within the range of their mean, plus or minus four-time standard deviation, 99.994% of the area beneath the normal density curve is covered. Thus, area correction will not be necessary. It should be noted that for choosing the initial data, the following conditions must be observed for the corrected CPT tip resistance and stress reduction factor:

$$\begin{cases} q_{c1N_{\min}} = q_{c1N_{\text{mean}}} - 4\sigma_{q_{c1N}} \geq 0 \\ r_{d_{\min}} = r_{d_{\text{mean}}} - 4\sigma_{r_d} \geq 0 \end{cases} \tag{37}$$

For reliability assessment of the liquefaction safety factor using the JDRV method, Eq. (11) is rewritten into terms of K_1 to K_7, as shown in Eq. (38). The terms K_1 to K_7 are introduced in Eq. (39). The probability density function of each term is derived separately by Eqs. (40) to (46). Derivations of these equations are presented below:

$$\text{FS}(K_1, K_2, K_3, K_4) = K_1.K_2.K_3.K_4 = K_5.K_3.K_4 = K_6.K_4 = K_7, \tag{38}$$

where:

$$\begin{cases} K_1 = L(q_{c1N}) \\ K_2 = \frac{1}{r_d} \\ K_3 = M_w^{-2.56} \\ K_4 = \frac{1}{\alpha} \\ K_5 = K_1 \times K_2 \\ K_6 = K_5 \times K_3 \\ K_7 = \text{FS} = K_6 \times K_4 \end{cases} \tag{39}$$

On the other hand:

$$f_{K_1}(k_1) = f_{q_{c1N}}(L^{-1}(k_1)) \times \left|\frac{dL^{-1}(k_1)}{dk_1}\right|$$

$$= f_{q_{c1N}}(q_{c1N}) \times \left|\frac{1}{\frac{dK_1}{dq_{c1N}}}\right|, \quad (40)$$

$$L(q_{c1N_{\max}}) \leq k_1 \leq L(q_{c1N_{\min}})$$

$$\begin{cases} k_{2_{\min}} = L(q_{c1N_{\max}}) \\ k_{2_{\max}} = L(q_{c1N_{\min}}) \end{cases}$$

$$f_{k_2}(k_2) = f_{r_d}(\frac{1}{k_2})\left|\frac{d}{dk_2}\left(\frac{1}{k_2}\right)\right| = \frac{1}{\sigma_{r_d}\sqrt{2\pi}.k_2^2}$$

$$\exp\left(-0.5\left(\frac{1-r_{d_{\mathrm{mean}}}.k_2}{\sigma_{r_d}.k_2}\right)^2\right), \quad (41)$$

$$r_{d_{\min}} \leq r_d \leq r_{d_{\max}} \quad \rightarrow \quad \frac{1}{r_{d_{\max}}} \leq k_2 \leq \frac{1}{r_{d_{\min}}}$$

$$\begin{cases} k_{2_{\min}} = \frac{1}{r_{d_{\max}}} \\ k_{2_{\max}} = \frac{1}{r_{d_{\min}}} \end{cases}$$

$$f_{K_3}(k_3) = f_{M_w}(k_3^{-\frac{25}{64}}) \times \left|\frac{d}{dk_3}(k_3^{(-\frac{25}{64})})\right|$$

$$= \frac{25 \times \lambda_{M_w}.\exp(-\lambda_{M_w} k_3^{-\frac{25}{64}})}{64 \times k_3^{(\frac{89}{64})}(\exp(-\lambda_{M_w} M_{w_{\min}}) - \exp(-\lambda_{M_w} M_{w_{\max}}))} \quad (42)$$

$$M_{w_{\min}} \leq M_w \leq M_{w_{\max}} \quad \rightarrow$$

$$(M_{w_{\max}})^{-2.56} \leq k_3 \leq (M_{w_{\min}})^{-2.56}$$

$$\begin{cases} k_{3_{\min}} = (M_{w_{\max}})^{-2.56} \\ k_{3_{\max}} = (M_{w_{\min}})^{-2.56} \end{cases}$$

$$f_{k_4}(k_4) = f_{\alpha}(\frac{1}{k_4})\left|\frac{d}{dk_4}\left(\frac{1}{k_4}\right)\right|$$

$$= \frac{\lambda_{\alpha}.\exp(\frac{-\lambda_{\alpha}}{k_4})}{k_4^2.\exp(-\lambda_{\alpha}.\alpha_{\min}) - \exp(-\lambda_{\alpha}.\alpha_{\max})} \quad (43)$$

$$\frac{1}{\alpha_{\max}} \leq k_4 \leq \frac{1}{\alpha_{\min}}$$

$$\begin{cases} k_{4_{\min}} = \frac{1}{\alpha_{\max}} \\ k_{4_{\max}} = \frac{1}{\alpha_{\min}} \end{cases}$$

$$f_{K_5}(k_5) = f_{K_1 \times K_2}(k_5)$$

$$= \int_{\alpha}^{\beta} |k_1| f_{K_1}(k_1) f_{K_2}\left(\frac{k_5}{k_1}\right) dk_1, \quad (44)$$

$$k_{1_{\min}} k_{2_{\min}} \leq k_5 \leq k_{1_{\max}} k_{2_{\max}}$$

$$\begin{cases} k_{5_{\min}} = k_{1_{\min}} k_{2_{\min}} \\ k_{5_{\max}} = k_{1_{\max}} k_{2_{\max}} \end{cases} \text{and :} \begin{cases} \alpha = \max[k_{1_{\min}} \& \frac{k_5}{k_{2_{\max}}}] \\ \beta = \min[k_{1_{\max}} \& \frac{k_5}{k_{2_{\min}}}] \end{cases}$$

$$f_{K_6}(k_6) = f_{K_5 \times K_3}(k_6) = \int_{\alpha}^{\beta} |k_3| f_{K_3}(k_3) f_{K_5}\left(\frac{k_6}{k_3}\right) dk_3, \quad (45)$$

$$k_{5_{\min}} k_{3_{\min}} \leq k_6 \leq k_{5_{\max}} k_{3_{\max}}$$

$$\begin{cases} k_{6_{\min}} = k_{5_{\min}} k_{3_{\min}} \\ k_{6_{\max}} = k_{5_{\max}} k_{3_{\max}} \end{cases} \text{and :} \begin{cases} \alpha = \max[k_{3_{\min}} \& \frac{k_6}{k_{5_{\max}}}] \\ \beta = \min[k_{3_{\max}} \& \frac{k_6}{k_{5_{\min}}}] \end{cases}$$

$$f_{K_7}(k_7) = f_{K_6 \times K_4}(k_7)$$

$$= \int_{\alpha}^{\beta} |k_4| f_{K_4}(k_4) f_{K_6}\left(\frac{k_7}{k_4}\right) dk_4, \quad (46)$$

$$k_{6_{\min}} k_{4_{\min}} \leq k_7 \leq k_{6_{\max}} k_{4_{\max}}$$

$$\begin{cases} k_{7_{\min}} = k_{6_{\min}} k_{4_{\min}} \\ k_{7_{\max}} = k_{6_{\max}} k_{4_{\max}} \end{cases} \text{and :} \begin{cases} \alpha = \max[k_{4_{\min}} \& \frac{k_7}{k_{6_{\max}}}] \\ \beta = \min[k_{4_{\max}} \& \frac{k_7}{k_{6_{\min}}}] \end{cases}$$

And the cumulative distribution function of K_7 can be determined as below:

$$F_{K_7}(k_7) = P\{K_7 \in [k_{7_{\min}}, k_7]\} = \int_{k_{7_{\min}}}^{k_7} f_{K_7}(t)dt$$

$$k_{7_{\min}} \leq k_7 \leq k_{7_{\max}}. \quad (47)$$

Using the above mathematical functions for K_1 to K_7 and $f_{K_1}(k_1)$ to $f_{K_7}(k_7)$, a computer program was developed (coded in MATLAB) to determine the probability density function curve of the liquefaction safety factor. In addition, for comparison, determination of the safety factor for liquefaction using Monte Carlo simulation was also coded in the same computer program. To show the ability of the proposed method, an example with arbitrary data is given in the following sections.

7. Example

To demonstrate the efficiency and accuracy of the proposed method in determining the probability density function curve for the liquefaction safety factor and reliability assessment, an example problem with selected parameter values from literature [2,3,60,69] is presented. In selecting, the following points are considered:

- The standard deviation of q_{c1N} was taken equal to 6, based on experience from different case history data.
- The standard deviation of r_d was selected based on the three-sigma rule [69] and the curve suggested by Seed and Idriss [1] for each depth.
- To consider the uncertainty of earthquake parameters, reasonable values were taken for the scale parameter of earthquake acceleration ratio and moment magnitude, equal to 0.05 and 0.8, respectively ($\beta_\alpha = 0.1$ and $\beta_{M_w} = 1.5$). Furthermore, the range of variation of α and M_w was taken as 0.2 and 2.5, respectively ($M_{w_{\max}} - M_{w_{\min}} = 2.5$ and $\alpha_{\max} - \alpha_{\min} = 0.2$).

The stochastic parameters with truncated normal and truncated exponential distributions are shown in Tables 1 and 2, respectively, and the deterministic parameters are given in Table 3.

The probability density functions of the stochastic parameters are shown in Figures 1 to 4. Moreover, in order to compare the results of the presented method with those of the Monte Carlo simulation, the final probability density and cumulative distribution curves for the factor of safety against liquefaction are determined using the same data and both methods. For this purpose, 1,000,000 generation points are used for the Monte Carlo simulation. The results are shown in Figures 5 and 6. As seen in these figures, the results obtained using the developed method are very close to that of the Monte Carlo simulation. The probability of liquefaction is shown by the blue region for FS < 1, in Figure 7. Figure 8 shows the cumulative distribution curve of the liquefaction safety factor. It can be seen that the probability of liquefaction (FS $\leq$ 1) for this site at the assessed depth (12 m) is about 67%. Table 4 indicates that liquefaction would most likely occur at this depth.

On the other hand, a deterministic calculation using the mean value of the stochastic parameters shows that the safety factor against liquefaction is about 0.8031. This demonstrates that, at this depth, liquefaction would occur, but the probability of liquefaction is not specified. Therefore, the designer cannot develop an engineering judgment. In fact, reliability assessment and engineering judgment are

Table 1. Stochastic truncated normal parameters.

Parameters	Mean	Standard deviation	Minimum	Maximum
r_d	0.8565	0.0207	0.7737	0.9394
q_{c1N}	80	6	56	104

Table 2. Stochastic truncated exponential parameters.

Parameters	λ	Minimum	Maximum	Mean	Standard
M_w	2/3	5.0	7.5	5.9179	0.6751
α	10	0.2	0.4	0.2687	0.05253

Table 3. Deterministic parameters.

Depth of water table (m)	Depth (m)	FC (%)	$\gamma_{d_{\min}}$ (kN/m^3)	$\gamma_{d_{\max}}$ (kN/m^3)	G_s
0.0	12.0	10.0	14.0	19.0	2.65

Table 4. Classes of liquefaction potential [70].

Probability	Class	Description (likelihood of liquefaction)
$0.85 < P_L < 1.00$	5	Almost certain that it will liquefy
$0.65 < P_L < 0.85$	4	Liquefaction very likely
$0.35 < P_L < 0.65$	3	Liquefaction and non-liquefaction equally likely
$0.15 < P_L < 0.35$	2	Liquefaction unlikely
$0.00 < P_L < 0.15$	1	Almost certain that it will not liquefy

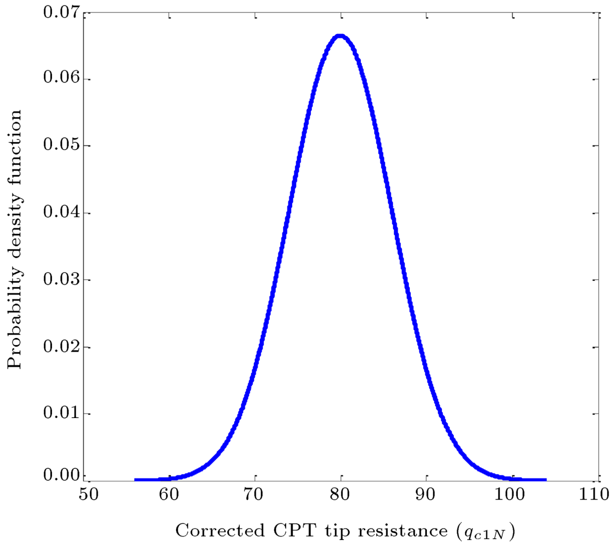

Figure 1. Probability density function of corrected CPT tip resistance.

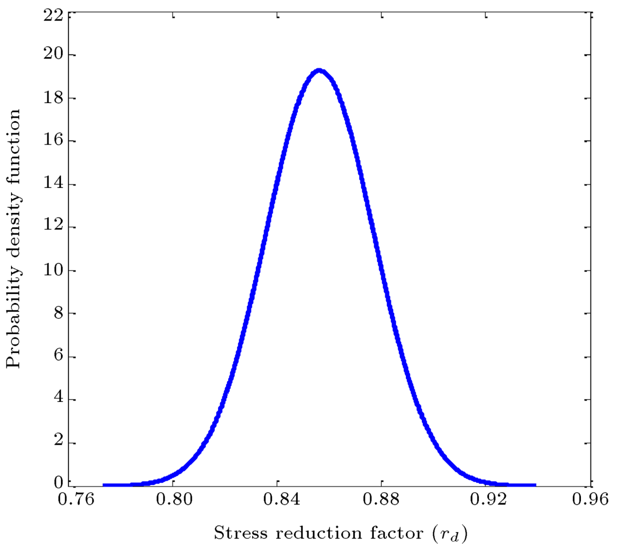

Figure 2. Probability density function of stress reduction factor.

employed together to develop risk and decision analyses.

For this example, a stepwise procedure for determining the probability density and cumulative distribution curves of the safety factor (Figures 5 and 6) from K_1 to K_7 by JDRV, and comparing them with Monte Carlo simulation, is presented in Appendix A.

8. Sensitivity analysis

To evaluate the response of the liquefaction potential (Eq. (1)) with respect to changes in input parameters, a sensitivity analysis was carried out by JDRV. For this purpose, all stochastic parameter pdf's were increased, based on their standard deviation (std). To evaluate

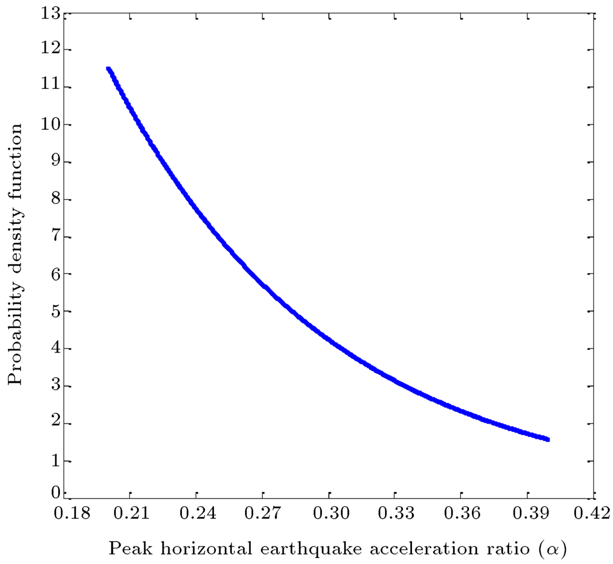

Figure 3. Probability density function of earthquake acceleration ratio.

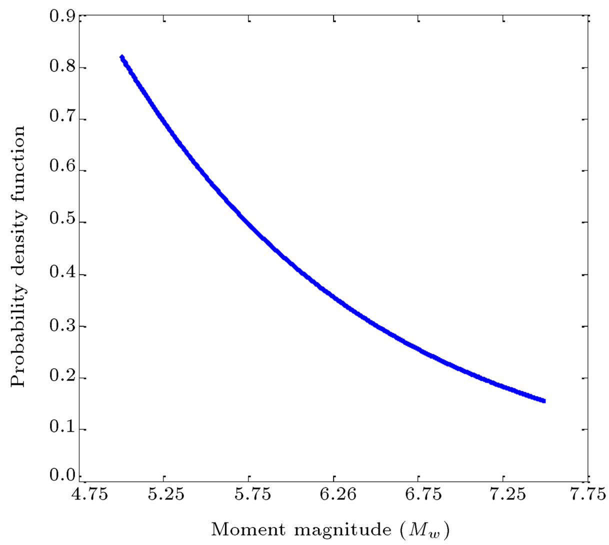

Figure 4. Probability density function of earthquake magnitude.

the influence of changes in the pdf of each stochastic parameter, that parameter was increased, while the ranges of the other stochastic input parameters were kept constant.

The results are shown in Figure 9. It is shown that, with an increase in the pdf of the corrected CPT tip resistance, the cumulative distribution function (cdf) of the safety factor shifts rightwards, indicating that a site with a higher value of density has a higher safety factor against liquefaction. Furthermore, Figure 9 shows that with an increase in earthquake acceleration ratio, moment magnitude and stress reduction factor, the cdf of liquefaction safety factor shifts leftwards, implying a decrease in the safety factor and an increase in the probability of liquefaction.

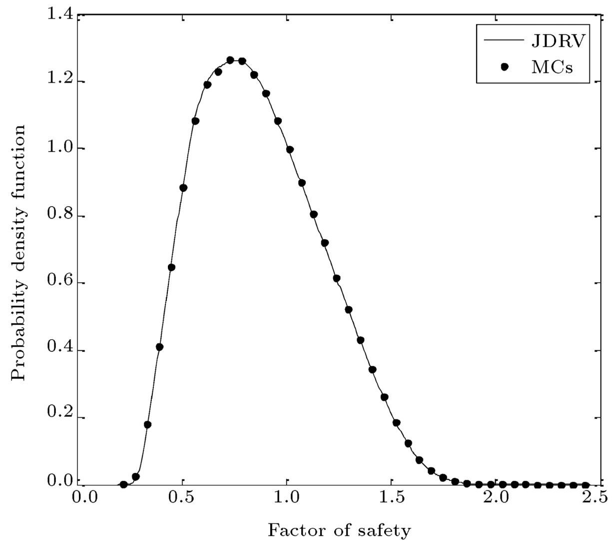

Figure 5. Comparison of probability density function of safety factor against liquefaction by two methods.

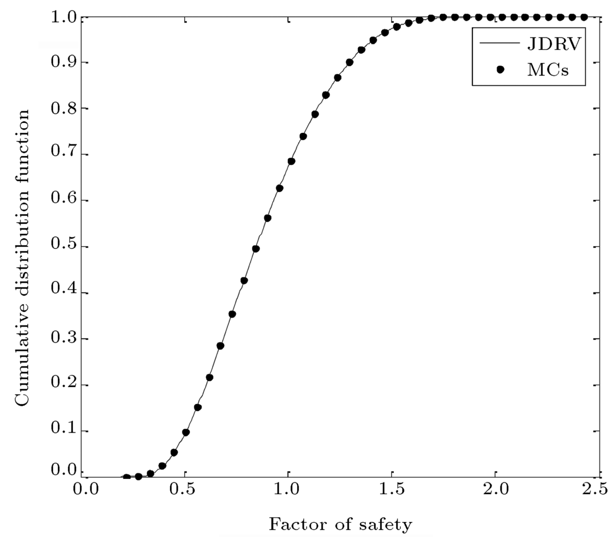

Figure 6. Comparison of cumulative distribution function of safety factor against liquefaction by two methods.

Table 5. The amounts of changes in probability of liquefaction corresponding to 1*std increase (shift rightward) in the pdf of parameters.

Stochastic parameter	Shift in the q_{c1N}	Shift in the r_d	Shift in the M_w	Shift in the α
Change (%)	-7.64	+2.37	+25.90	+18.45

Based on Figure 9, the amounts of shift in the curves (change in probability of liquefaction) corresponding to 1*std increase in the pdf of the stochastic parameters, with respect to the original pdf for FS = 1, are given in Table 5. This table shows that the moment magnitude is the most effective parameter in the safety factor of liquefaction.

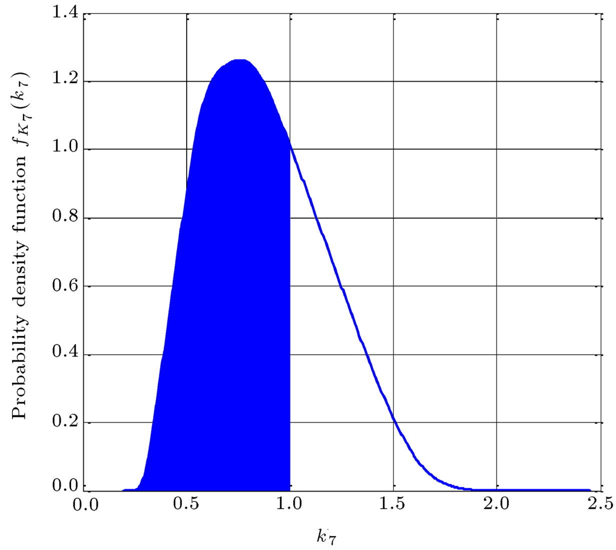

Figure 7. Probability of liquefaction in the example using probability density function.

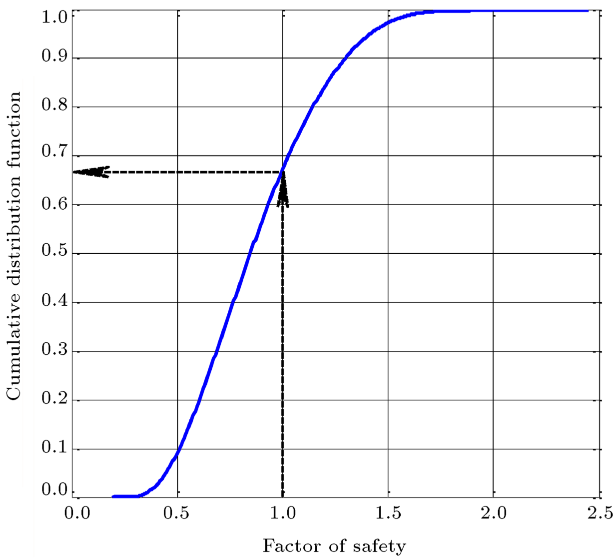

Figure 8. Probability of liquefaction in the example using cumulative distribution function.

Figure 10 shows the effect of depth on safety factor against liquefaction. It can be seen that by increasing depth, the cumulative distribution function shifts rightward, indicating a decrease in the probability of liquefaction. The selected depths and the corresponding calculated probability of liquefaction are shown in this figure.

9. Parametric analysis

For further verification of the proposed method, a parametric analysis is performed. The main goal is to find the effect of each parameter on the probability of liquefaction. Figure 11 presents the determined values of the probability of liquefaction (FS=1 on cdf) as

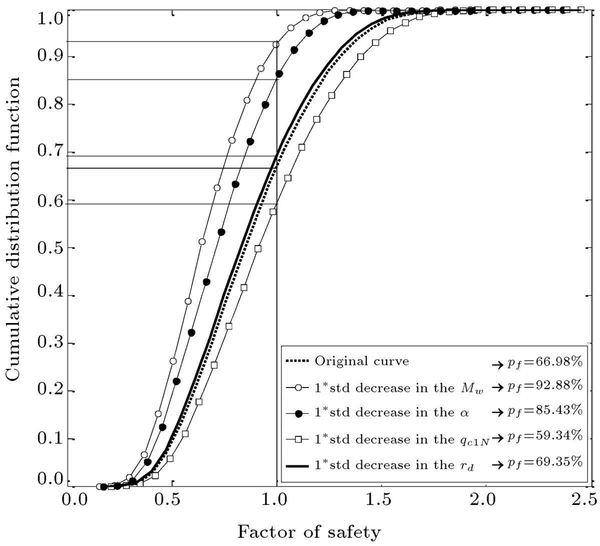

Figure 9. Sensitivity analysis to determine the response of model and the most effective parameter.

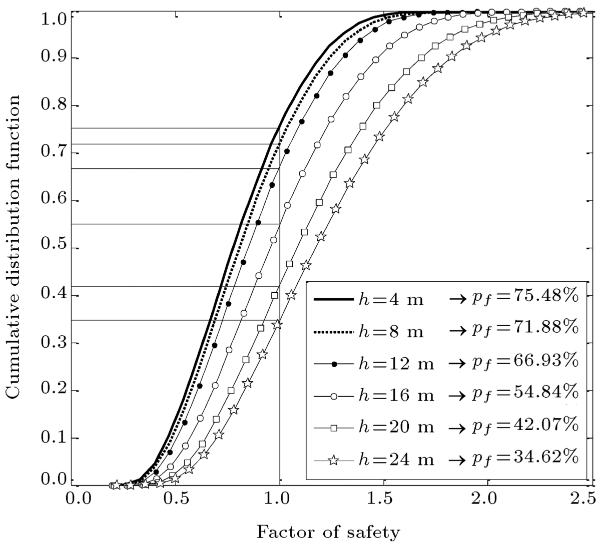

Figure 10. Depth effect assessment in safety factor against liquefaction.

a function of each parameter, where others are constant. For this purpose, in seven steps, the probability density function of each stochastic input parameter is increased based on their standard deviation (new pdf = old pdf + 1/3 × std). The results of the parametric analysis indicate that, as expected, the probability of liquefaction continuously increases due to the shift rightward of the probability density function of earthquake magnitude, earthquake acceleration ratio and stress reduction factor, based on their standard deviation. This assessment shows that the moment magnitude is the most effective parameter in reduction of the safety factor of liquefaction. Figure 11 shows the probability of liquefaction decreases when the corrected CPT tip resistance increases.

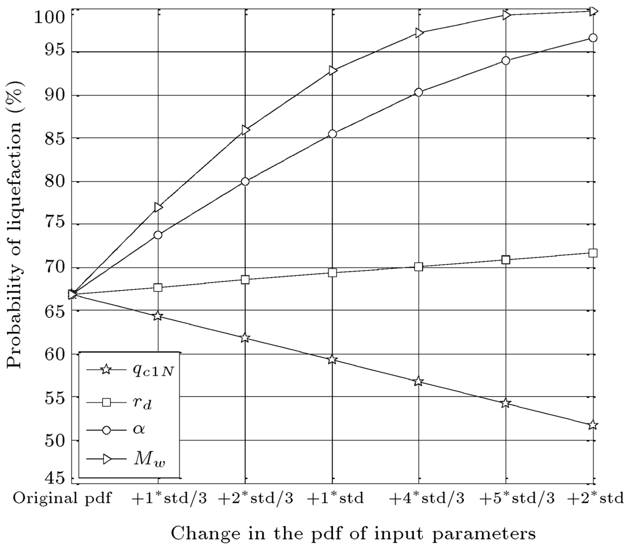

Figure 11. Parametric analysis of probability of liquefaction with respect to change of probability distribution function of input parameters.

10. Conclusion

Determination of liquefaction potential is a probabilistic problem due to the inherent uncertainties in estimation of both earthquake characteristics and the heterogeneous nature of soils. Uncertainties in earthquake characteristics can be evaluated using standard probabilistic seismic analysis, and uncertainties in soil parameters can be assessed in terms of the uncertainties in geotechnical parameters or model performance, as well as human uncertainty. In this paper, the jointly distributed random variable method is used to assess the reliability of the safety factor for liquefaction. The selected stochastic parameters are the corrected CPT tip resistance and stress reduction factor, which are modeled using truncated normal probability density functions, and the earthquake acceleration ratio and moment magnitude, which are considered to have truncated exponential probability density functions. The results show that the determined probability distribution of liquefaction safety factor by the JDRV method is very close to that predicted by the Monte Carlo simulation. In addition, the sensitivity analysis of the selected method indicates that this method can correctly predict the patterns of influence of the stochastic parameters. The sensitivity analysis also shows that the moment magnitude is the most effective parameter in the safety factor against liquefaction. Moreover, the results indicate that the JDRV method is able to capture the expected probability distribution of the safety factor of liquefaction correctly. Furthermore, the parametric analysis shows an acceptable trend for the probability of liquefaction with changing the input parameters. This method can be used as an analytical tool in assessment of the reliability of liquefaction potential.

References

1. Seed, H.B. and Idriss, I.M. "Simplified procedure for evaluating soil liquefaction potential", *Journal of the Soil Mechanics and Foundations Division, ASCE*, **97**(SM9), pp. 1249-1273 (1971).
2. Kramer, S.L. *Geotechnical Earthquake Engineering*, Prentice Hall (1996).
3. Youd, T.L. and Idriss, I.M. "Liquefaction resistance of soils: Summary report from the 1996 NCEER and 1998 NCEER/NSF workshop on evaluation of liquefaction resistance of soils", *Journal of Geotechnical and Geoenvironmental Engineering, ASCE*, **127**(4), pp. 297-313 (2001).
4. Seed, H.B., Tokamatsu, K., Harder, L.F. and Chung, R. "The influence of SPT procedure on soil liquefaction resistance evaluations", *Rep. No. UCB/EERC-84/15, Earthquake Engg. Res Ctr.*, University of California, Berkeley, Calif (1984).
5. Seed, H.B., Tokimatsu, K., Harder Jr, L.F. and Chung, R. "Influence of SPT procedures in soil liquefaction resistance evaluations", *Journal of Geotechnical Engineering, ASCE*, **111**(12), pp. 861-878 (1985).
6. Seed, H.B. and De Alba, P.M. "Use of SPT and CPT Tests for evaluating the liquefaction resistance of sands", *Proc., INSITU '86, ASCE Spec. Conf. on Use of In Situ Testing in Geotechnical Engg. Spec. Publ.*, No. **6**, ASCE, New York, N.Y. (1986).
7. Seed, R.B. and Harder Jr, L.F. "SPT-based analysis of cyclic pore pressure generation and undrained residual strength", *Proc.*, H.B. Seed Memorial Symp., BiTech Publishing, Vancouver, B.C., Canada, **2**, pp. 351-376 (1990).
8. Arulndandan, K., Yogachandran, C., Meegoda, N.J., Ying, L. and Zhauji, S. "Comparision of the SPT, CPT, SV and electrical methods of evaluating earthquake induced liquefaction susceptibility in Ying Kou city during the Haicheng earthquake", *Proc., Use of In Situ Tests in Geotech. Engrg., Geotech. Spec. Publ.*, **6**, ASCE, New York, N.Y., pp. 389-415 (1986).
9. Mitchell, J.K. and Tseng, D.J. "Assessment of liquefaction potential by cone penetration rresistance", *Proc., H.B. Seed Memorial Symp.*, **2**, BiTech Publishing, Vancouver, B.C., Canada, pp. 335-350 (1990).
10. Robertson, P.K. "Cone penetration testing for evaluating liquefaction potential", *Proc., Symp. on Recent Advances in Earthquake Des. Using Lab. and In Situ Tests*, ConeTec Investigations Ltd., Burnaby B.C., Canada (1990).
11. Baziar, M.H. and Nilipour, N. "Evaluation of liquefaction potential using neural-networks and CPT results", *Soil Dynamics and Earthquake Engineering*, **23**(7), pp. 631-636 (2003).
12. Robertson, P.K. and Wride, C.E. "Evaluating cyclic liquefaction potential using the cone penetration test", *Canadian Geotechnical Journal*, **35**, pp. 442-459 (1998).
13. Juang, C.H. and Chen, C.J. "CPT-based liquefaction evaluation using artificial neural networks", *Computer-Aided Civil and Infrastructure Engineering*, **14**(3), pp. 221-229 (1999).
14. Juang, C.H., Yuan, H.M., Lee, D.H. and Lin, P.S. "Simplified cone penetration test-based method for evaluating liquefaction resistance of soils", *Journal of Geotechnical and Geoenvironmental Engineering*, **129**(1), pp. 66-80 (2003).
15. Idriss, I.M. and Boulanger, R.W. "Semi-empirical procedures for evaluating liquefaction potential during earthquakes", *Soil Dynamics and Earthquake Engineering*, **26**, pp. 115-130 (2006).
16. Andrus, R.D. and Stokoe II, K.H., "Liquefaction resistance based on shear wave velocity", *Proceedings of NCEER Workshop on Evaluation of Liquefaction Resistance of Soils* (1997).
17. Andrus, R.D. and Stokoe II, K.H. "Liquefaction resistance of soils from shear-wave velocity", *Journal of Geotechnical and Geoenvironmental Engineering*, **126**(11), pp. 1015-1025 (2000).
18. Morgenstern, N.R., "Managing risk in geotechncial engineering", *Proceeding of the 10th Pan American Conference on Soil Mechanic and Foundation Engineering*, **4**, pp. 102-126 (1995).
19. Griffiths, D.V. and Fenton, G.A., *Probabilistic Methods in Geotechnical Engineering*, Springer Wien NewYork (2007).
20. Whitman, V.W., "Organizing and evaluating uncertainty in geotechnical engineering, in uncertainty in geologic environment: From theory to practice", *Proceedings of Uncertainty '96*, Geotechnical Special Publication, ASCE, **58**(1), pp. 1-38 (1996).
21. Sowers, G.S. "The human factor in failure", *Civil Engineering, ASCE*, **61**(3), pp. 72-73 (1991).
22. Johari, A., Javadi, A.A., Makiabadi, M.H. and Khodaparast, A.R. "Reliability assessment of liquefaction potential using the jointly distributed random variables method", *Soil Dynamics and Earthquake Engineering*, **38**, pp. 81-87 (2012).
23. Johari, A. and Khodaparast, A.R. "Modelling of probability liquefaction based on standard penetration tests using the jointly distributed random variables method", *Engineering Geology*, **158**, pp. 1-14 (2013).
24. Ang, A.H.S. and Tang, W.H. *Probability Concepts in Engineering Planning and Design*, **I**, John Wiley and Sons, New York, USA (1984).
25. Rosenblueth, E. "Point estimates for probability moments", *Proceedings*, National Academy of Science, **72**(10), pp. 3812-3814 (1975).

26. Hasofer, A.M. and Lind, N.C. "An exact and invariant first-order reliability format", *Journal of the Engineering Mechanics Division*, **100**(EM1), pp. 111-121 (1974).

27. Haldar, A. and Tang, W.H. "Probabilistic evaluation of liquefaction potential", *Journal of the Getechnical Engineering Division, ASCE*, **105**(2), pp. 145-163 (1979).

28. Fardis, M.N. and Veneziano, D. "Probabilistic analysis of deposit liquefaction", *Journal of Geotechnical and Geoenvironmental Engineering, ASCE*, **108**(3), pp. 395-417 (1982).

29. Chameau, J.L. and Clough, G.W. "Probabilistic pore pressure analysis for seismic loading", *Journal of Geotechnical Engineering, ASCE*, **109**(4), pp. 507-524 (1983).

30. Juang, C.H., Rosowsky, D.V. and Tang, W.H. "Reliability-based method for assessing liquefaction potential of soils", *Journal of Geotechnical and Geoenvironmental Engineering*, **125**(8), pp. 684-689 (1999).

31. Juang, C.H., Yang, S.H., Yuan, H. and Khor, E.H. "Characterization of the uncertainty of the Robertson and Wride model for liquefaction potential evaluation", *Soil Dynamics and Earthquake Engineering*, **24**, pp. 771-780 (2004).

32. Hwang, J.H., Yang, C.W. and Juang, D.S. "A practical reliability-based method for assessing soil liquefaction potential", *Soil Dynamics and Earthquake Engineering*, **24**, pp. 761-770 (2004).

33. Juang, C.H., Yang, S.H. and Yuan, H. "Model uncertainty of shear wave velocity-based method for liquefaction potential evaluation", *Journal of Geotechnical and Geoenvironmental Engineering, ASCE*, **131**(10), pp. 1274-1282 (2005).

34. Lee, Y.F., Chi, Y.Y., Lee, D.H., Juang, C.H. and Wu, J.H. "Simplified models for assessing annual liquefaction probability – A case study of the Yuanlin area. Taiwan", *Engineering Geology*, **90**, pp. 71-88 (2007).

35. Jha, S.K. and Suzuki, K. "Liquefaction potential index considering parameter uncertainties", *Engineering Geology*, **107**, pp. 55-60 (2009).

36. Jha, S.K. and Suzuki, K. "Reliability analysis of soil liquefaction based on standard penetration test", *Journal of Computers and Geotechnics*, **36**, pp. 589-596 (2009).

37. Lee, Y.F., Chi, Y.Y., Juang, C.H. and Lee, D.H. "Annual probability and return period of soil liquefaction in Yuanlin, Taiwan attributed to Chelungpu fault and Changhua fault", *Engineering Geology*, **114**, pp. 343-353 (2010).

38. Metropolis, N. and Ulam, S. "The Monte Carlo method", *Journal of the American Statistical Association*, **44**(247), pp. 335-341 (1949).

39. Popescu, R., Prevost, J.H. and Deodatis, G. "3D effects in seismic liquefaction of stochastically variable soil deposits", *Geotechnique*, **55**(1), pp. 21-31 (2005).

40. Lopez-Caballero, F. and Modaressi-Farahmand-Razavi, A. "Assessment of variability and uncertainties effects on the seismic response of a liquefiable soil profile", *Soil Dynamics and Earthquake Engineering*, **30**, pp. 600-613 (2010).

41. Fenton, G.A. and Vanmarcke, E.H. "Spatial variation in liquefaction risk", *Geotechnique*, **48**(6), pp. 819-831 (1998).

42. Christian, J.T. and Swiger, W.F. "Statistic of liquefaction and SPT result", *Journal of the Geotechnical Engineering Division, ASCE*, **101**(11), pp. 1135-1150 (1975).

43. Yegian, M.K. and Whitman, R.V. "Risk analysis for ground failure by liquefaction", *Journal of the Geotechnical Engineering Division, ASCE*, **104**(7), pp. 921-938 (1978).

44. Veneziano, D. and Liao, S. "Statistical analysis of liquefaction data", *Proceedings, 4th ASCE Specialty conference on Probabilistic Mechanics and Structural Reliability*, pp. 206-209 (1984).

45. Liao, S.S.C., Veneziano, D. and Whitman, R.V. "Regression models for evaluating liquefaction probability", *Journal of Geotechnical Engineering, ASCE*, **114**(4), pp. 389-411 (1988).

46. Papathanassiou, G. "LPI-based approach for calibrating the severity of liquefaction-induced failures and for assessing the probability of liquefaction surface evidence", *Engineering Geology*, **96**, pp. 94-104 (2008).

47. Juang, C.H., Chen, C.J., Tang, W.H. and Rosowsky, D.V. "CPT-based liquefaction analysis, Part 1: Determination of limit state function", *Geotechnique*, **50**(5), pp. 583-592 (2000).

48. Juang, C.H., Chen, C.J., Rosowsky, D.V. and Tang, W.H. "CPT-based liquefaction analysis, Part 2: Reliability for design", *Geotechnique*, **50**(5), pp. 593-599 (2000).

49. Juang, C.H., Chen, C.J., Tang, W.H. and Rosowsky, D.V. "CPT-based liquefaction analysis, Part 1: Determination of limit state function", *Geotechnique*, **50**(5), pp. 583-592 (2000).

50. Juang, C.H., Chen, C.J. and Jiang, T. "Probabilistic framework for liquefaction potential by shear wave velocity", *Journal of Geotechnical and Geoenvironmental Engineering*, **127**(8), pp. 670-678 (2001).

51. Juang, C.H., Fang, S.Y. and Khor, E.H. "First-order reliability method for probabilistic liquefaction trig-

gering analysis using CPT", *Journal of Geotechnical and Geoenvironmental Engineering*, **132**(3), pp. 337-350 (2006).

52. Chern, S.G., Lee, C.Y. and Wang, C.C. "CPT-based liquefaction assessment by using fuzzy-neural network", *Journal of Marine Science and Technology*, **16**(2), pp. 139-148 (2008).

53. Idriss, I.M. and Boulanger, R.W. "Soil liquefaction during earthquake", *Earthquake Engineering Research Institute*, EERI Publication MNO-12 (2008).

54. Liao, S. and Whitman, R.V. "Overburden correction factors for SPT in sand", *Journal of Geotechnical Engineering*, **112**(3), pp. 373-377 (1986).

55. Idriss, I.M. "Earthquake ground motions at soft soil sites", *Proc., 2nd Int. Conf. on Recent Advances in Geotechnical Earthquake Engineering and Soil Dynamics*, **3**, pp. 2265-2271 (1991).

56. Andrus, R.D., Piratheepan, P., Ellis, B.S., Zhang, J. and Juang, C.H. "Comparing liquefaction evaluation methods using penetration-VS relationships", *Soil Dynamics and Earthquake Engineering*, **24**(9-10), pp. 713-721 (2004).

57. Terzaghi, K. and Peck, R.B. *Soil Mechanics in Engineering Practice*, 2nd Edn., John Wiley, NY (1967).

58. Tokimatsu, K. and Seed, H.B. "Evaluation of settlements in sands due to earthquake shaking", *Journal of Geotechnical Engineering*, **113**(8), pp. 861-878 (1987).

59. Cubrinovski, M. and Ishihara, K. "Empirical correlation between SPT N-value and relative density for sandy soils", *Soils and Foundations*, **39**(5), pp. 61-71 (1999).

60. Das, B.M. *Advanced Soil Mechanics*, 3rd Edn.Taylor & Francis (2008).

61. Hoel, P.G., Port, S.C. and Stone, C.J. "Introduction to probability theory", *Houghton Mifflin*, Boston, MA (1971).

62. Tijms, H. *Understanding Probability*, 2nd Ed., Cambridge University Press (2007).

63. Ramachandran, K.M. and Tsokos, C.P., *Mathematical Statistics with Applications*, Elsevier Academic Press (2009).

64. Johari, A. and Javadi, A.A. "Reliability assessment of infinite slope stability using the jointly distributed random variables method", *Scientia Iranica*, **19**(3), pp. 423-429 (2012).

65. Johari, A., Fazeli, A. and Javadi, A.A. "An investigation into application of jointly distributed random variables method in reliability assessment of rock slope stability", *Journal of Computers and Geotechnics*, **47**, pp. 42-47 (2013).

66. Johari, A., Javadi, A.A., Elmi, M. and Raei, S. "An analytical approach to reliability assessment of the shear wave velocity relationship", *Scientia Iranica*, **20**(6), pp. 1685-1694 (2013).

67. Johari, A. and Khodaparast, A.R. "Modelling of probability liquefaction based on standard penetration tests using the jointly distributed random variables method", *Engineering Geology*, **158**, pp. 1-14 (2013).

68. Hahn, G.J. and Shapiro. S.S. *Statistical Models in Engineering*, New York: Wiley (1967).

69. Duncan, J.M. "Factors of safety and reliability in geotechnical engineering", *Journal of Geotechnical and Geoenvironmental Engineering, ASCE*, **126**(4), pp. 307-316 (2000).

70. Juang, C.H., Jiang, T. and Andrus, R.D. "Assessing probability-based methods for liquefaction potential evaluation", *Journal of Geotechnical and Geoenvironmental Engineering, ASCE*, **128**(7), pp. 580-589 (2002).

Appendix A

In this Appendix, for the demonstrated example, a stepwise procedure for determining probability density and the cumulative distribution curves of the safety factor against liquefaction (Figures 5 and 6) are presented. The JDRV method and MC simulation results of the coded computer program for the pdf of K_1 to K_7 are shown in Figures A.1 to A.7.

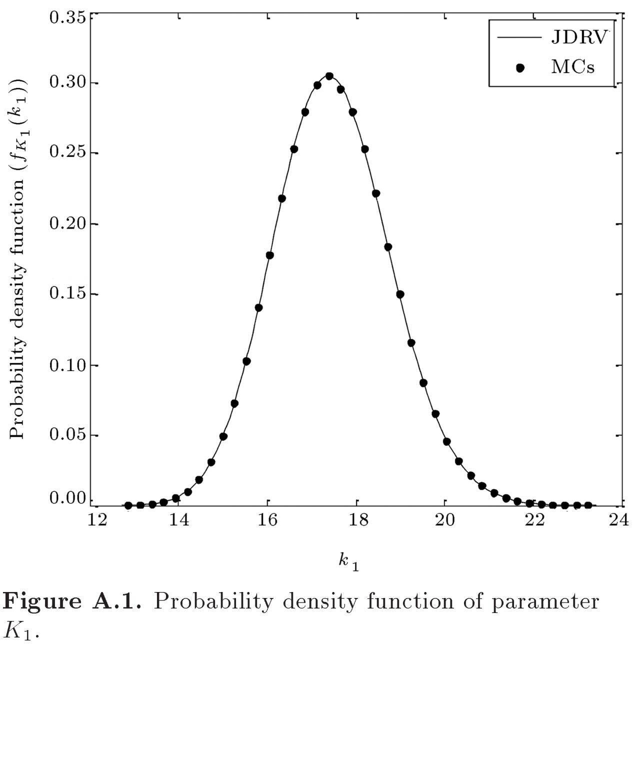

Figure A.1. Probability density function of parameter K_1.

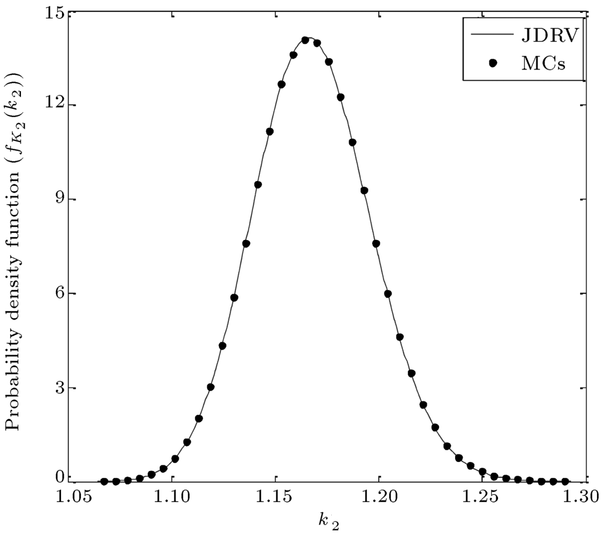

Figure A.2. Probability density function of parameter K_2.

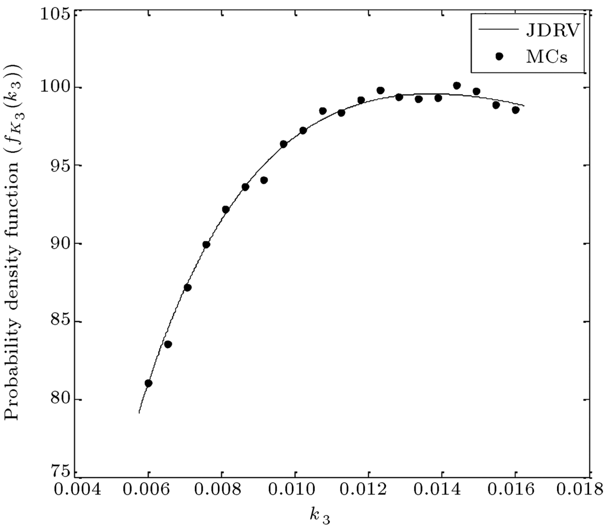

Figure A.3. Probability density function of parameter K_3.

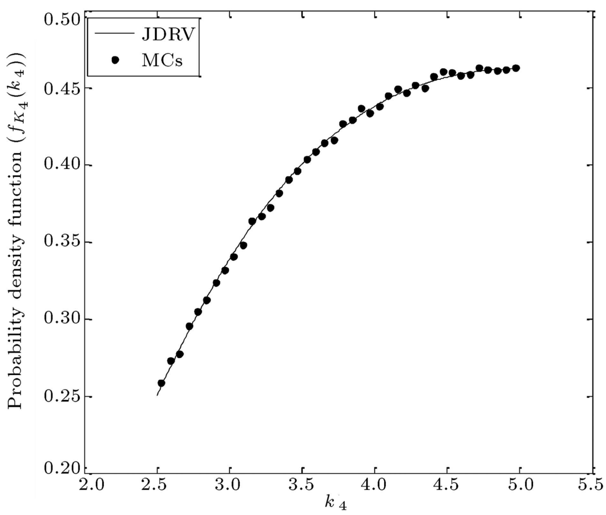

Figure A.4. Probability density function of parameter K_4.

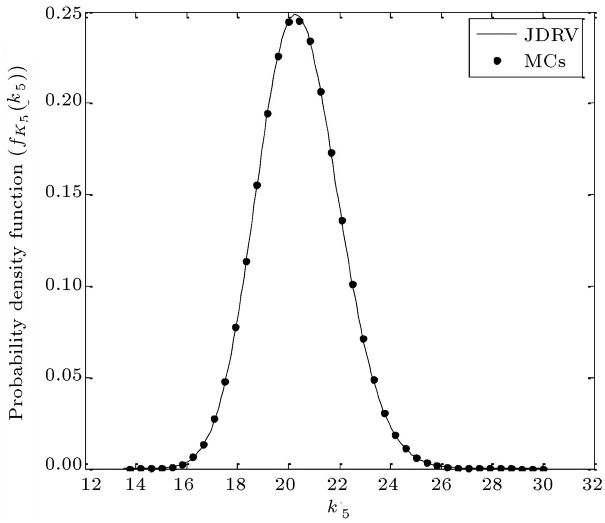

Figure A.5. Probability density function of parameter K_5.

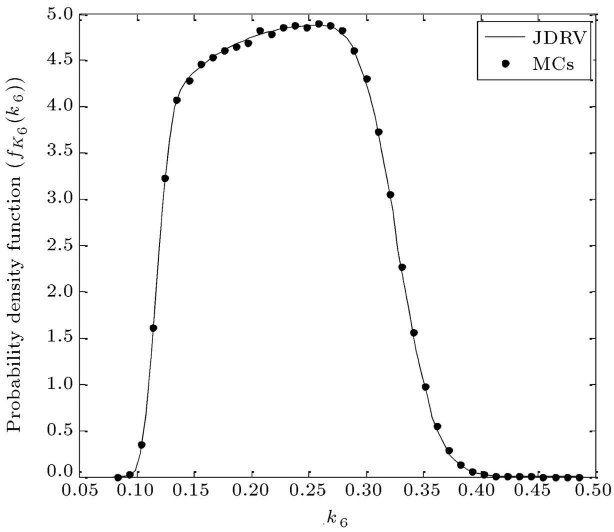

Figure A.6. Probability density function of parameter K_6.

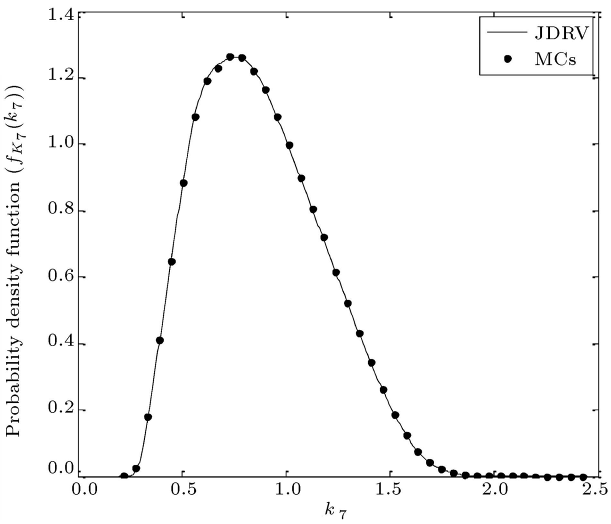

Figure A.7. Probability density function of parameter K_7.

Biographies

Ali Johari obtained his BS, MS and PhD degrees in 1995, 1999 and 2006, respectively, from Shiraz University, Iran, where he is currently Assistant Professor in the Civil and Environmental Engineering Department. He was a Post-Doctoral Researcher at Exeter University in 2008, where he is also a member of the research staff of the Computational Geomechanics Group. His research interests include unsaturated soil mechanics, application of intelligent systems in geotechnical engineering, probabilistic analysis and reliability assessment. He has also consulted and supervised numerous geotechnical projects.

Alireza Khodaparast received his MS degree from Shiraz University of Technology, Iran, in 2012. His research interests include reliability analysis. At present, he is involved in various civil engineering projects.